Mathematical and Computational Applications, Vol. 20, No. 3, pp. 174-188, 2015
http://dx.doi.org/10.19029/mca-2015-015

SPINNING FLOW OF CASSON FLUID NEAR AN INFINITE ROTATING DISK

Najeeb Alam Khan[1] and Zehra Husain[2]

[1]Department of Mathematical Sciences, University of Karachi, 75270, Karachi, Pakistan
[2]College of Computer Science and Information System, Institute of Business Management, 75190, Karachi, Pakistan
[1]njbalam@yahoo.com

Abstract- This paper presents an investigation of the spinning flow of a non-Newtonian Casson fluid over a rotating disk. The model established for the governing problem in the form of partial differential equations has been converted to ordinary differential equations with the use of suitable similarity transformation. The analytical approximation has been made with the most likely analytical method, homotopy analysis method (HAM). The convergence region of the obtained solution is determined and plotted. The velocity profiles are shown and the influence of Casson parameter is discussed in detail. Also comparison has been made with the Newtonian fluid as the special case of considered problem.

Keywords- Casson fluid, rotating disk, Non-Newtonian, homotopy analysis method (HAM)

1. INTRODUCTION

The Newton's expression of viscosity can be infringed by such fluids which comprise many deferments such as shampoo, coal-water or coal-oil slurries, toothpaste, clay covering, postponements, oil, skin-deep products, custard, dyes, yoghurt, tomato paste, body fluid, emollients, toners, dyes, superglues, detergents, and sludge etc. The performance of these kind of fluids cannot be characterized by classical Navier–Stokes equations and having non-linear stress–strain relationship, which is known as non-Newtonian fluid. The flows of such fluids are handled extensively in polymer processing and chemical engineering processes. Rheological characteristics of non-Newtonian fluids are used in biological and biomedical devices like homodialyser. Usually in non-Newtonian fluid models, the constitutive non-linear stress-strain relations receive difficulties that lead to nonlinear equations of motion. Irrespective of composite and nonlinear model, the presentations of non-Newtonian fluids have concerned the interest of the investigators. The constitutive expression between stress and shear rate is not able to addressed all the non-Newtonian fluids. From Casson [1], Casson fluid is also a type of non-Newtonian fluid. Casson fluid exhibits yield stress; it is well known that Casson fluid is a clipcontraction liquid. At zero rate of shear, it is having an infinite viscosity. Casson fluids are of different types. Some are in plasma form for example jelly and blood. However, some fluids are like thick viscous form like honey, tomato soup, concentrated fruit juices, shampoo etc. from the study of Dash et al [2].Venkatesam et al. [3] studied about blood rheology in stenosed narrow arteries by in view of blood as a Casson fluid and compared their results with the Herschel-Bulkley fluid model. Bhattacharyya et al. [4] perform a numerical computation to investigate the phenomena of heat transfer and the effect of thermal radiation over a stretching sheet for a two-dimensional magnetohydrodynamic (MHD) stagnation-point flow of electrically performing non-Newtonian Casson fluid. In his study, he observed that the velocity boundary layer thickness is better for Casson fluid as compared to facilitate of Newtonian fluid, also by increasing the values of velocity ratio parameter the heat transfer rate is increased too. Sankar et al. [5] performed a comparative analysis between Herschel Bulkley fluid and Casson fluid representation by considering the pulsatile flow of blood in slender conical arteries with gentle extend beyond stenosis. The study revealed that mean velocity and mean flow rate have higher values in Herschel Bulkley fluid model as measure up to Casson model, while the plug core radius and wall shear stress, lower values in Herschel Bulkley fluid model as compared to Casson model. Paszynski et al. [6] modified the Fluid Particle Model (FPM) in which the study used the non- linear constitutive equation and show the possibilities to suggest the flow of blood as a Casson fluid, also the transport coefficients for the modified FPM can be significantly useful for representation of stream of blood expressed by non-linear Casson constitutive law.

Benton [7] started discussion about rotational flow over a disk with great effort. About the spinning flow near an infinite rotating disk eventually Rajagopal [8] studied about the swirling flows related to viscoelastic fluids. However the effort was done by Attia[9] later on involving unvarying suction or injection of the fluid nearby a spinning permeable disk which was basically unstable MHD flow. Erdogan [10] studied the flow which was induced and implemented in a non-torsional fluctuation and a rotation of fluid infinitely by non-coaxial disk revolution. Anderson et al. [11] returned power-law fluid flow to a completed spinning disk. Takhar et al [12] worked on unstable flow of MHD and the transfer of heat over a moving disk and the fluid was ambient. Cheng and Liao [13] worked on the analytical solution of Von Kármán about the spinning of viscous flow in the obvious and decent way. Turkyilmazoglu[14-15] did the remarkable effort upon the work on revolution of disk regarding exact solutions which showed the resemblance to the glutinous incompressible and leading fluid. He also studied about the compressible boundary layer flow over morally investigative resolutions having heat transfer in arrears to a porous moving disk. Later on the study was done by Turkyilmazoglu[16] on MHD boundary layer flow as well which again involved the roughness on the moving disk. Meanwhile Sibanda et al. [17-18] discussed the problem about osmic heating and viscous indulgence on MHD flow and the transfer of heat effectively on a porous medium over a moving disk. The work was continued with other problem going on Spectral-homotopy analysis solutions as well. Attempt was made exclusively well by Khan et al. [19-21] recently worked in which the problems were taken under consideration about the unstable MHD flow of couple stress as well as Powell Eyring fluids. He also did the study in the same manner on Jeffery fluid over an off-centered moving disk.

The main purpose of this chapter is to learn about spinning flow of Casson fluid over a rotating disk in occurrence of external magnetic field. It may be because of the mathematical complexity of this particular model. The resulting nonlinear equations of Cassonfluids are more complicated than the Navier-Stokes equation. The flow equations obtained by the use of a second order approximation of the Casson model. The homotopy analysis method is the main technique which is used to get analytical solution. Graphs are also represented showing the physical behavior of evolving parameters in a clear manner.

2. MATHEMATICAL MODEL

Here we are considering three dimensional, laminar, steady, incompressible, flow of Casson fluid in a semi-bounded. By taking r,θ and z axes along radial, tangential and axial direction and assume that the uniform magnetic field B is acting along the z-axis. The flow geometry of the considered problem presented as Fig. 1.

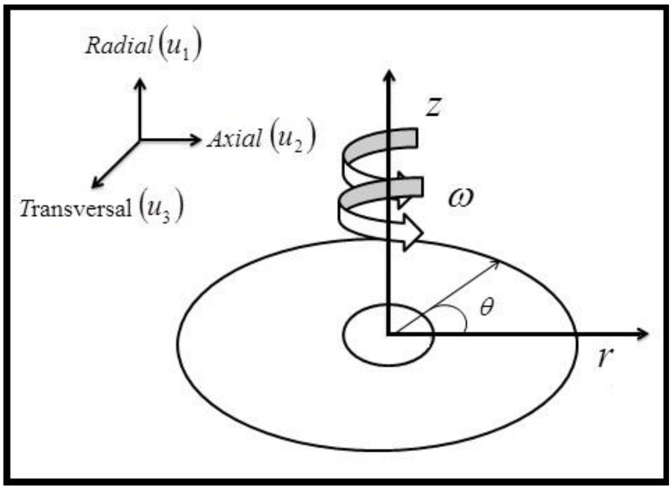

Figure 1. Physical model and flow alignment.

The constitutive equation for Casson model can be shown as.

$$\boldsymbol{S} = -p\boldsymbol{I} + \boldsymbol{T} \tag{1}$$

Where $\boldsymbol{S}$ is the Cauchy stress tensor, $\boldsymbol{T}$ is the extra stress tensor, $\boldsymbol{I}$ is the identity tensor, p is the pressure and shear stress flow of a Casson fluid is given by

$$T_{ij} = \begin{cases} 2\left(\mu_B + \dfrac{p_y}{\sqrt{2\pi}}\right)e_{ij}, & \pi > \pi_c \\ 2\left(\mu_B + \dfrac{p_y}{\sqrt{2\pi_c}}\right)e_{ij}, & \pi < \pi_c \end{cases}, \tag{2}$$

As discussed in previous chapter $\pi = e_{ij}e_{ij}$ and e_{ij} is the $(i,j)^{th}$ factor of the twist rate. Where μ the coefficient of is shear viscosity and $\beta = \dfrac{\mu_B\sqrt{2\pi_c}}{p_y}$ is the Casson fluid parameter.

Now consider the velocity and stress as

$$\boldsymbol{u}=\left(u_1,u_2,u_2\right)\ ,\ \boldsymbol{T}(r)=\begin{pmatrix}\boldsymbol{T}_{11} & \boldsymbol{T}_{12} & \boldsymbol{T}_{13}\\ \boldsymbol{T}_{21} & \boldsymbol{T}_{22} & \boldsymbol{T}_{23}\\ \boldsymbol{T}_{31} & \boldsymbol{T}_{32} & \boldsymbol{T}_{33}\end{pmatrix} \tag{3}$$

$$T_{11}=\left(\mu_B+\frac{p_y}{\sqrt{2\pi}_c}\right)2\left(\frac{\partial u_1}{\partial r}\right) \tag{4}$$

$$T_{12}=T_{21}=\left(\mu_B+\frac{p_y}{\sqrt{2\pi}_c}\right)\left(\frac{\partial u_2}{\partial r}+\frac{1}{r}\frac{\partial u_1}{\partial \theta}-\frac{u_2}{r}\right) \tag{5}$$

$$T_{13}=T_{31}=\left(\mu_B+\frac{p_y}{\sqrt{2\pi}_c}\right)\left(\frac{\partial u_1}{\partial z}+\frac{\partial u_3}{\partial r}\right) \tag{6}$$

$$T_{22}=\left(\mu_B+\frac{p_y}{\sqrt{2\pi}_c}\right)2\left(\frac{1}{r}\frac{\partial u_2}{\partial \theta}+\frac{u_1}{r}\right) \tag{7}$$

$$T_{23}=T_{32}=\left(\mu_B+\frac{p_y}{\sqrt{2\pi}_c}\right)\left(\frac{1}{r}\frac{\partial u_3}{\partial \theta}+\frac{\partial u_2}{\partial z}\right) \tag{8}$$

$$T_{33}=\left(\mu_B+\frac{p_y}{\sqrt{2\pi}_c}\right)2\left(\frac{\partial u_3}{\partial z}\right) \tag{9}$$

By using the above equations, we get the continuity, the momentum and energy equations which can be written as:

$$\frac{\partial u_1}{\partial r}+\frac{u_1}{r}+\frac{1}{r}\frac{\partial u_2}{\partial \theta}+\frac{\partial u_3}{\partial z}=0 \tag{10}$$

$$\rho\left(u_1\frac{\partial u_1}{\partial r}-\frac{u_2^{\,2}}{r}-\frac{u_2}{r}\frac{\partial u_1}{\partial \theta}+u_3\frac{\partial u_1}{\partial z}\right)=-\partial_r p+\left(\partial_r T_{11}+\partial_z T_{31}+\frac{1}{r}\partial_\theta T_{12}+\frac{\left(T_{11}-T_{22}\right)}{r}\right) \tag{11}$$

$$\rho\left(u_1\,\partial_r u_2+\frac{u_1\,u_2}{r}+\frac{u_2}{r}\frac{\partial u_2}{\partial \theta}+u_3\,\partial_z u_2\right)=\left(\partial_r T_{12}+\partial_z T_{32}+2\frac{T_{12}}{r}+\frac{\partial_\theta T_{22}}{r}\right) \tag{12}$$

$$\rho\left(u_1\,\partial_r u_3+\frac{u_2}{r}\frac{\partial u_3}{\partial \theta}+u_3\,\partial_z u_3\right)=-\partial_z p+\left(\partial_r T_{13}+\partial_z T_{33}+\frac{T_{13}}{r}+\frac{\partial_\theta T_{23}}{r}\right) \tag{13}$$

By using the boundary conditions on the disk and the boundary conditions at infinity

$$u_1(0)=0,\qquad u_2(0)=r\,\Omega,\quad u_3(0)=0,\ u_1(\infty)=0,\ u_3(\infty)=0 \tag{14}$$

Here the similarity transformations will be:

$$u_1 = r\,\omega\,F(\eta),\quad u_2 = r\,\omega\,G(\eta),\; u_3 = \sqrt{\nu\,\omega}\,H(\eta),\; p = \rho\,\nu\,\omega\,P(\eta),\; \eta = \sqrt{\frac{\omega}{\nu}}\,z\,,\, Re = \frac{\omega\,r^2}{\nu}, \quad (15)$$

After using the above similarity transformation we get the following equations

$$\left(1+\frac{1}{\beta}\right)F''(\eta) - F(\eta)^2 + G(\eta)^2 - H(\eta)F'(\eta) = 0, \quad (16)$$

$$\left(1+\frac{1}{\beta}\right)G''(\eta) - H(\eta)G'(\eta) - 2F(\eta)G(\eta) = 0, \quad (17)$$

$$H(\eta)H'(\eta) - P'(\eta) - \left(1+\frac{1}{\beta}\right)H''(\eta) = 0\,, \quad (18)$$

But Eqs. (11) yields the relation

$$F(\eta) = \frac{-H'(\eta)}{2} \quad (19)$$

Substituting Eq. (19) into Eqs. (16)-(8), we have

$$\left(1+\frac{1}{\beta}\right)H'''(\eta) - H''(\eta)\,H(\eta) + \frac{1}{2}\left(H'(\eta)\right)^2 - 2G^2(\eta) = 0, \quad (20)$$

$$\left(1+\frac{1}{\beta}\right)G''(\eta) - H(\eta)\,G'(\eta) + G(\eta)\,H'(\eta) = 0, \quad (21)$$

with boundary conditions at $\eta = 0$ and $\eta = \infty$

$$H(0) = H'(\infty) = H'(0) = 0,\quad G(0) = 1,\quad G(\infty) = 0, \quad (22)$$

Where F, H and G are the radial, axial and tangential components of dimensionless velocity and P is the dimensionless pressure of the flow.

By substituting $\beta = \dfrac{\mu_B\sqrt{2\pi_c}}{p_y}$ and $Re = \dfrac{\omega\,r^2}{\nu}$, the shear stresses of the Casson fluid in radial and axial directions can be calculated as:

$$T_{13} = T_{31} = \left(\mu_B + \frac{p_y}{\sqrt{2\pi_c}}\right)\left(r\,\nu\,\omega\sqrt{\frac{\omega}{\nu}}\right)\left(F'(\eta)\right)$$

$$= \mu_B\left(1+\frac{1}{\beta}\right)\left(-\frac{1}{2}\nu\,\omega\sqrt{\mathrm{Re}}\,H''(\eta)\right) \quad (23)$$

$$T_{23} = T_{32} = \left(\mu_B + \frac{p_y}{\sqrt{2\pi}_c} \right) \left(r\, \nu\, \omega \sqrt{\frac{\omega}{\nu}} \right) \left(G'(\eta) \right)$$
$$= \mu_B \left(1 + \frac{1}{\beta} \right) \left(\nu\, \omega \sqrt{\mathrm{Re}}\, G'(\eta) \right) \tag{24}$$

Therefore, the local skin-friction coefficients are given by:

$$C_F = \mu_B \left(1 + \frac{1}{\beta} \right) \left(-\frac{1}{2} \frac{1}{\sqrt{\mathrm{Re}}} H''(\eta) \right) \tag{25}$$

and $C_G = \mu_B \left(1 + \frac{1}{\beta} \right) \frac{1}{\sqrt{\mathrm{Re}}} G'(\eta)$ (26)

3. SOLUTION OF THE PROBLEM

The homotopy analysis method (HAM) presented by Liao [22-23] is used to obtain the analytical solutions. HAM is a very powerful technique to find analytical solutions as it provides huge flexibility to choose the convergence region with the help of convergence control parameter $\hbar$ and it has been successfully used to been solved by this method [24-25].

By means of HAM the following initial estimation $H_0(\eta)$, $G_0(\eta)$ have been chosen to understand the comprehensive and totally analytic solutions of Eqs.(20)-(21) with the boundary conditions (22), its shown as:

$$H_0 = -1 + e^{-\eta}(1+\eta), \quad G_0 = e^{-\eta} \tag{27}$$

Here $\mathcal{L}_1$and $\mathcal{L}_2$ are the auxiliary linear operators

$$\mathcal{L}_1(H) = H''' + H'' \tag{28}$$

$$\mathcal{L}_2(G) = G'' - G \tag{29}$$

The following properties are persuaded by,

$$\mathcal{L}_1\left[\mathrm{c}_1 \mathrm{e}^{\eta} + \mathrm{c}_2 + \eta\, \mathrm{c}_3\right] = 0 \tag{30}$$

$$\mathcal{L}_2\left[\mathrm{c}_4 \mathrm{e}^{\eta} + \mathrm{c}_5\, \mathrm{e}^{-\eta}\right] = 0 \tag{31}$$

The zeroth –order deformation equations are

$$(1-\varepsilon)\mathcal{L}_1\left[\overline{H}(\eta,\varepsilon) - \overline{H}_0(\eta)\right] = \varepsilon\, \hbar\, N_1\left[\overline{H}(\eta,\varepsilon), \overline{G}(\eta,\varepsilon)\right] \tag{32}$$

$$(1-\varepsilon)\mathcal{L}_2\left[G(\eta,\varepsilon) - \overline{H}_0(\eta)\right] = \varepsilon\, \hbar\, N_2\left[H(\eta,\varepsilon), \overline{G}(\eta,\varepsilon)\right] \tag{33}$$

The boundary conditions for this deformation are

$$H(\eta,0)-H_0(\eta)=0,\quad H(\eta,1)-H(\eta)=0 \tag{34}$$

$$G(\eta,0)-G_0(\eta)=0,\quad G(\eta,1)-G(\eta)=0 \tag{35}$$

Based on Eqs. (32)-(33), N_1 and N_2 are the non-linear operators which can be defined by

$$N_1=\left(1+\frac{1}{\beta}\right)\frac{\partial^3\overline{H}(\eta,\varepsilon)}{\partial\eta^3}-\overline{H}(\eta,\varepsilon)\,\frac{\partial^2\overline{H}(\eta,\varepsilon)}{\partial\eta^2}+\frac{1}{2}\left(\frac{\partial\overline{H}(\eta,\varepsilon)}{\partial\eta}\right)^2-2\,\overline{G}(\eta,\varepsilon)^2 \tag{36}$$

$$N_2=\left(1+\frac{1}{\beta}\right)\frac{\partial^2\overline{G}(\eta,\varepsilon)}{\partial\eta^2}-\overline{H}(\eta,\varepsilon)\left(\frac{\partial\overline{G}(\eta,\varepsilon)}{\partial\eta}\right)+\overline{G}(\eta,\varepsilon)\left(\frac{\partial\overline{H}(\eta,\varepsilon)}{\partial\eta}\right) \tag{37}$$

As we know that $\varepsilon\in[0,1]$is the embedding parameter and $\hbar$ is the auxiliary nonzero parameter. By Taylor's theorem,

$$H(\eta,\varepsilon)=H_0(\eta)+\sum_{m=1}^{\infty}H_m(\eta)\varepsilon^m,\quad H_m(\eta)=\frac{1}{m!}\frac{\partial^m H(\eta,\varepsilon)}{\partial\varepsilon^m}\Big|_{\varepsilon=0} \tag{38}$$

$$G(\eta,p)=G_0(\eta)+\sum_{m=1}^{\infty}G_m(\eta)\varepsilon^m,\quad G_m(\eta)=\frac{1}{m!}\frac{\partial^m G(\eta,\varepsilon)}{\partial\varepsilon^m}\Big|_{\varepsilon=0} \tag{39}$$

The series Eqs. (38) - (39) are convergent at $\varepsilon=1$and hence Eqs. (34)-(35) yields because the values of $\hbar$ are selected in such a manner that

$$H(\eta)=H_0(\eta)+\sum_{m=1}^{\infty}H_m(\eta) \tag{40}$$

$$G(\eta)=G_0(\eta)+\sum_{m=1}^{\infty}G_m(\eta) \tag{41}$$

The deformation problems are

$$\mathcal{L}_1\left[H_m(\eta,\varepsilon)-\chi_m H_{m-1}(\eta)\right]=\hbar\,R_m(\eta) \tag{42}$$

$$\mathcal{L}_2\left[G_m(\eta,\varepsilon)-\chi_m G_{m-1}(\eta)\right]=\hbar\,Q_m(\eta) \tag{43}$$

$$H_m(0)=H_m'(\infty)=H_m'(0)=0,\quad G_m(0)=0,\quad G_m(\infty)=0, \tag{44}$$

Where,

$$R_m=\left(1+\frac{1}{\beta}\right)H'''_{m-1}-\sum_{i=0}^{m-1}H''_i\,H_{m-1-i}-2\sum_{i=0}^{m-1}G_iG_{m-1-i}+\frac{1}{2}\sum_{i=0}^{m-1}H'_i\,H'_{m-1-i},$$

$$Q_m=\left(1+\frac{1}{\beta}\right)G''_{m-1}-\sum_{i=0}^{m-1}H_iG'_{m-1-i}+\sum_{i=0}^{m-1}H'_i\,G_{m-1-i},$$

and

$$\chi_m = \begin{cases} 0, & m \le 1 \\ 1, & m > 1 \end{cases}$$

The symbolic computation software MATHEMATICA has been used for the solution of Eqs. (42)-(43) with boundary conditions (44).

4. DISCUSSION OF THE GRAPHICAL RESULTS

The $\hbar$ graphs are computed for $F''(\eta), G'(\eta), P'(\eta)$ and $H'(\eta)$ to achieve the convergence region and the acceptable range of values for different values of rotational and Casson parameters as depicted in Figs. 2-3. Fig. 4 shows the dimensionless velocity profiles for Casson fluid. It displays the effect of Casson parameter β on the profiles of the radial velocity, tangential velocity, axial velocity and pressure. The radial component of velocity rises near the disk and then slowly reduces to zero, allowing more fluid to pass from the disk, the tangential component of velocity decays exponentially, and the axial component of velocity has the asymptotic limiting value.

By means of observation from Fig. 5, it is quite clear that an increase in Casson parameter β decreases the dimension less constituent of radial velocity F over the rotational disk. Fig. 6 demonstrates that an increases in Casson parameter show the way to an increase in tangential velocity component G at any known tangential location on top of the revolving disk. Fig. 7 shows that an increase in the Casson parameter decreases the axial velocity H. Fig. 8 explains that there is a reduction in pressure with the increase in Casson parameter β. Later on Fig. 9-12 illustrates the comparison of the result between homotopy analysis method (HAM) and Runge-Kutta method (RKM) which also verifies the result. Also, the table shows the comparison of numerical values calculated by HAM from the values taken from White [26] for viscous fluid.

Table 1. The mathematical explanation for Casson fluid parameter $\beta = 0.1$ and for viscous flow i.e. for $\beta \to \infty$. Bracket values are of $\beta \to \infty$ i.e. of viscous fluids from White [26].

η	F	F'	G	G'	H	$-P$
0	0.0 (0.0)	0.510474 (0.51023)	1.0 (1.0000)	-0.623153 (-0.61592)	0.0 (-0.0)	0.0 (0.0)
0.1	0.0467425 (0.0462)	0.397923 (0.4163)	0.93921 (0.9386)	0.604691 (-0.6112)	-0.00410004 (-0.0048)	0.095501 (0.0924)
0.2	0.0833887 (0.0836)	0.316175 (0.338)	0.826776 (0.8780)	-0.582508 (-0.5987)	-0.0153538 (-0.0179)	0.171451 (0.1674)
0.3	0.1266 (0.1133)	0.2558 (0.2620)	0.822154 (0.8190)	-0.55778 (-0.5803)	-0.0323507 (-0.0377)	0.231499 (0.2274)
0.4	0.13645 (0.1364)	0.2103559 (0.1999)	0.767683 (0.7621)	-0.53144 (-0.5577)	-0.053874 (-0.0628)	0.278024 (0.2747)
0.5	0.156084 (0.1536)	0.175464 (0.1467)	0.715895 (0.7075)	-0.504228 (-0.5321)	-0.0788806 (-0.0919)	0.313282 (0.3115)
0.6	0.172505 (0.1660)	0.126216 (0.1015)	0.666847 (0.6557)	-0.476719 (-0.5047)	-0.106481 (-0.1239)	0.339343 (0.3396)
0.7	0.18639 (0.1742)	0.108339 (0.0635)	0.620546 (0.6067)	-0.449358 (-0.4763)	-0.135922 (-0.1580)	0.358041 (0.3608)
0.8	0.198232 (0.1789)	0.0434545 (0.0317)	0.576959 (0.5605)	-0.422482 (-0.4476)	-0.16657 (-0.1933)	0.370958 (0.3764)
0.9	0.208394 (0.1807)	0.00808339 (0.0056)	0.536025 (0.5171)	-0.39634 (-0.4191)	-0.197896 (-0.2293)	0.379432 (0.3877)
1.0	0.217151 (0.1801)	-0.0198 (-0.0157)	0.497661 (0.4766)	-0.371112 (-0.3911)	-0.229464 (-0.2655)	0.384562 (0.3955)
∞	0.0 (0.0)	-0.0 (-0.0)	0.0 (0.0)	-0.0 (-0.0)	-0.836136 (-0.8838)	0.364850 (0.3906)

5. CONCLUDING REMARKS

In this study, an effort has been made to investigate the spinning flow of a non-Newtonian Casson fluid over a rotating disk. The governing partial differential equations were transformed into ordinary differential equations by means of a suitable similarity transformation. The analytical solution of the governing equations was obtained by homotopy analysis method and the obtained results were compared with the Newtonian fluid as a special case of the considered problem. Results obtained in this study showed an excellent agreement with results presented in [26]. The influence of Casson fluid parameter was also observed on the velocity profiles in radial, tangential, and axial directions; and pressure distribution.

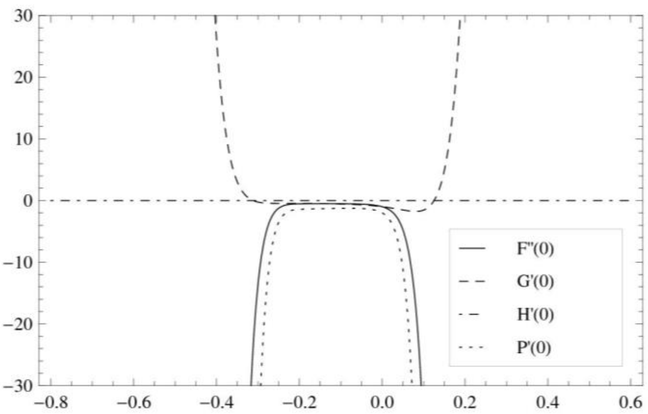

Figure 2. The $\hbar$ curves for $F''(0)$, $G'(0)$, $H'(0)$ and $P'(0)$ for $\beta = 1$.

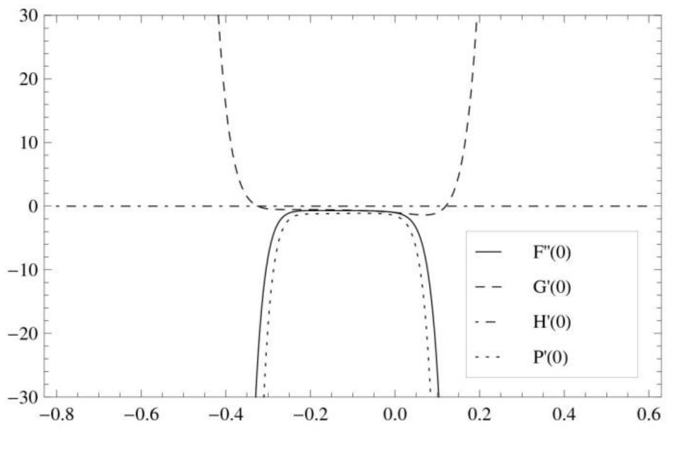

Figure 3. The $\hbar$ curves for $F''(0)$, $G'(0)$, $H'(0)$ and $P'(0)$ for $\beta = 2$.

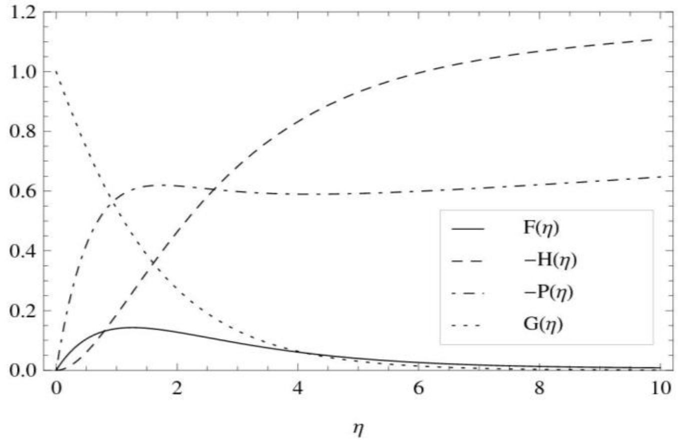

Figure 4. Dimensionless velocity and pressure profile for Casson fluid

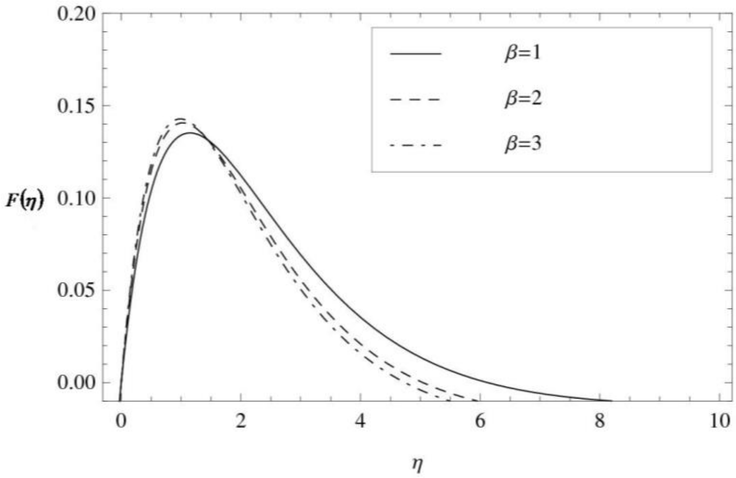

Figure 5. The radial velocity component F .

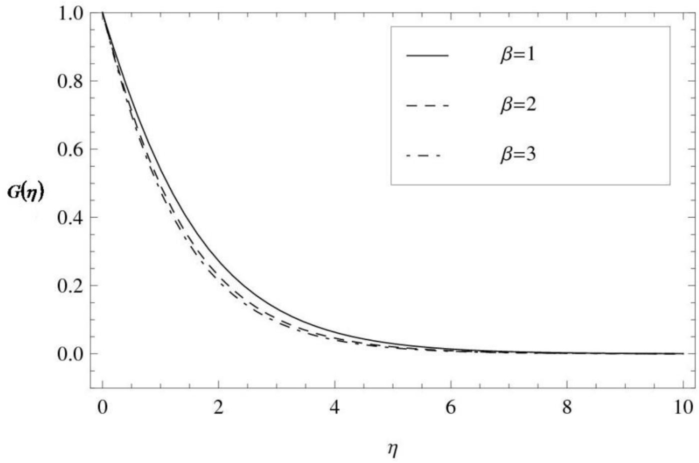

Figure 6. The tangential velocity component G .

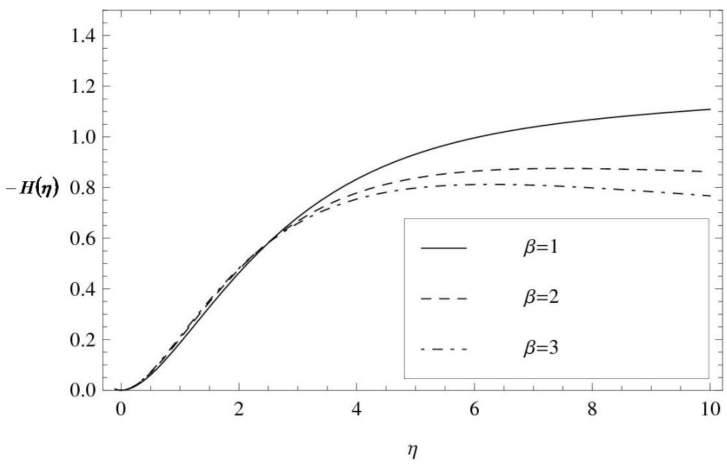

Figure 7. The axial velocity component H .

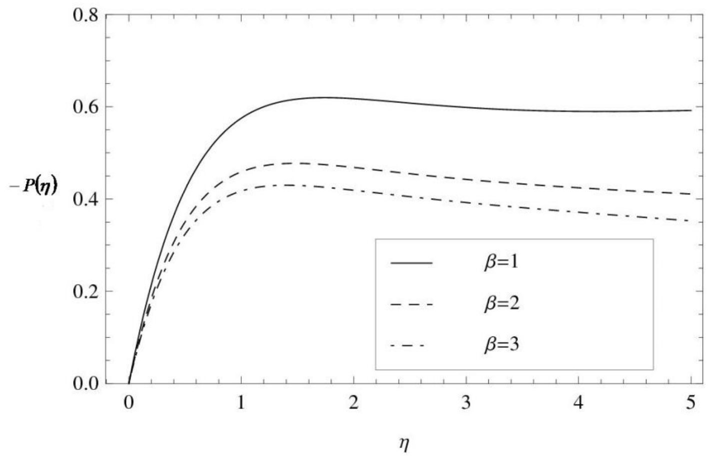

Figure 8. The pressure function P .

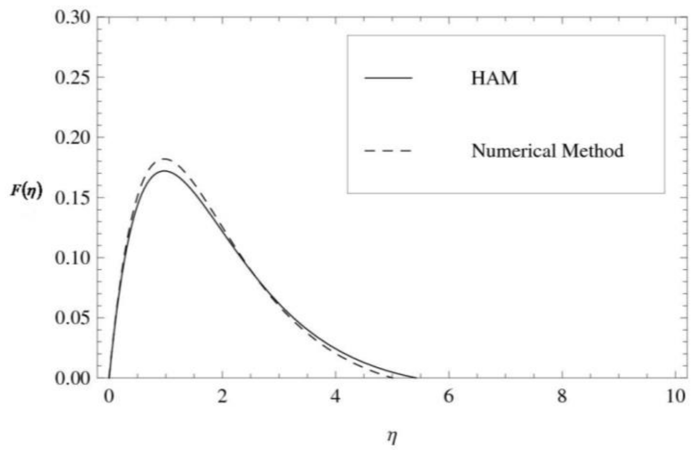

Figure 9. Comparison of the result with HAM and RK Method on $F(\eta)$ for $\beta = 1$, $\hbar = -0.05$

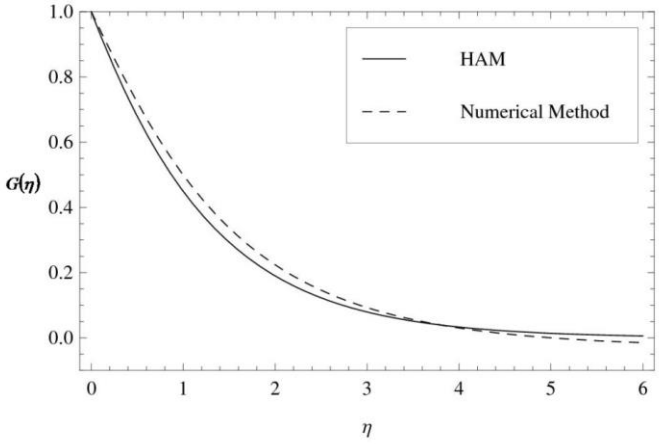

Figure 10. Comparison of the result with HAM and RK Method on $G(\eta)$ for $\beta = 1$, $\hbar = \text{-}0.1$

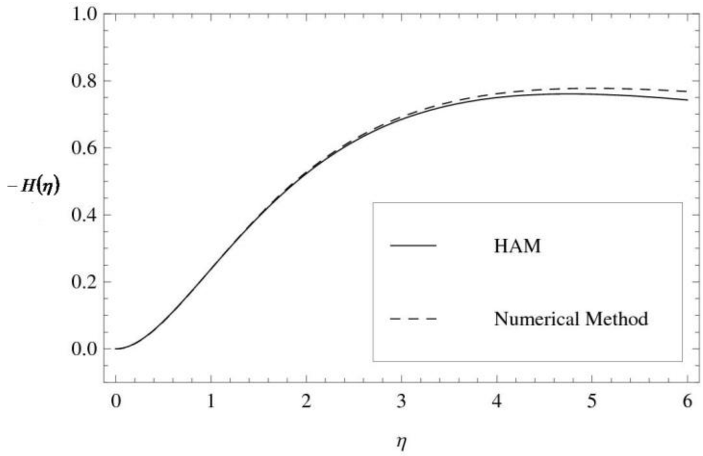

Figure 11. Comparison of the result with HAM and RK Method on $-H(\eta)$ for $\beta = 1$, $\hbar = \text{-}0.05$

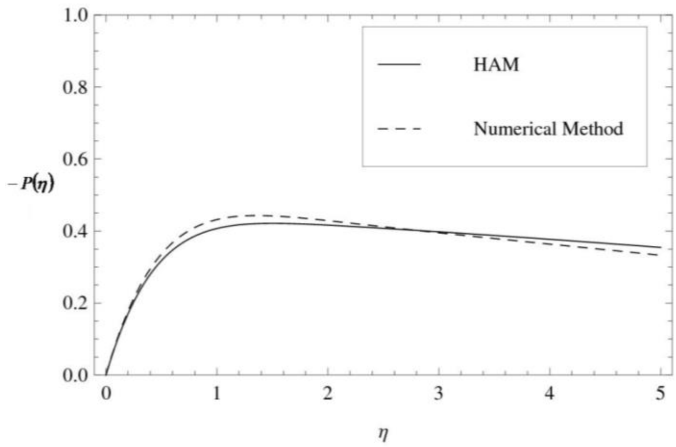

Figure 12. Comparison of the result with HAM and RK Method on $-P(\eta)$ for $\beta = 1$, $\hbar = \text{-}0.05$

6. REFERENCES

1. N. Casson, In rheology of dispersed system (Edited by C.C. MILL), *Pergamon Press*, Oxford, 1959.
2. R. K. Dash, K. N. Mehta, and G. Jayaraman, Casson fluid flow in a pipe filled with a homogeneous porous medium. *International Journal of Engineering Science,* **34**, 1145-56, 1996.
3. J. Venkatesan, D. S. Sankar, K. Hemalatha and Y. Yatim, Mathematical analysis of Casson fluid model for blood rheology in stenosed narrow arteries, *Journal of Applied Mathematics*, Article ID 583809, 2013.
4. K. Bhattacharyya, MHD stagnation-point flow of Casson fluid and heat transfer over a stretching sheet with thermal radiation, *Journal of Thermodynamics,* Article ID 169674, 2013.
5. D. S. Sankar, and Y. Yatim, Comparative analysis of mathematical models for blood flow in tapered constricted arteries, *Abstract and Applied Analysis,* Article ID 235960, 2012.
6. M. Paszynski, and R. Schaefer, The modified fluid particle model for non-linear Casson fluid and its parallel distributed implementation, *Computational Methods Applied Mechanical Engineering,* **194**, 4386-4410, 2005.
7. E. T. Benton, On the flow due to a rotating disk, *Journal of Fluid Mechanics*, **24**, 781-800, 1966.
8. K. R. Rajagopal, Swirling flows of viscoelastic fluids, *International Journal of Engineering Science,* **30**, 143-149, 1988.
9. H. A. Attia, Unsteady MHD flow near a rotating porous disk with uniform suction or injection, *Fluid Dynamics Research,* **23**, 283-290, 1998.
10. M. E. Erdogan, Flow induced by non-coaxial rotation of a disk executing non-torsional oscillation and a fluid rotating at infinity, *International Journal of Engineering Science,* **38**, 175-196, 2000.
11. H. I. Anderson, E. de Korte, R. Meland, Flow of a power-law fluid over a rotating disk revisited, *Fluid Dynamics Research*, **28**, 75-88, 2001.
12. H. S. Takhar, A. K. Singh, and G. Nath, Unsteady MHD flow and heat transfer on a rotating disk in an ambient fluid, *International Journal Thermal Science,* **41**, 147-155, 2002.
13. Y. Cheng, and S. J. Liao, On the explicit, purely analytic solution of von Kármán swirling viscous flow, *Communication Nonlinear Science Numerical Simulation*, **11**, 75-85, 2006.
14. M. Turkyilmazoglu, Exact solutions corresponding to the viscous incompressible and conducting fluid flow due to rotating disk, ZAMM-Journal of Applied Mathematics and Mechanics, **89**, 490-503, 2009.
15. M. Turkyilmazoglu, Purely analytic solutions of the compressible boundary layer flow due to a porous rotating disk with heat transfer, *Physics of fluids,* Article ID 106104-12, 2009.
16. M. Turkyilmazoglu, The MHD boundary layer flow due to a rough rotating disk, *ZAMM-Journal of Applied Mathematics and Mechanics,* **90**, 72-82, 2010.

17. P. Sibanda, and O. D. Makinde, On MHD flow and heat transfer past a rotating disk in porous medium with Ohmic heating and viscous dissipation, *International Journal of Numerical Methods Heat Fluid Flow*, **20**, 269-285, 2010.
18. P. Sibanda, and A. A. Khidar, On Spectral-homotopy analysis solutions of steady magnetohydrodynamic (MHD) flow and heat transfer from a rotating disk in a porous medium, *Scientific Research and Essays*, **7**, 2770-2780, 2012.
19. N. A. Khan, S. Aziz and N. Khan, Numerical simulation for the unsteady MHD flow of couple stress fluid over a rotating disk, *PLOS ONE,* **9,** e95423, 2014.
20. N. A. Khan, S. Aziz and N. Khan, MHD flow of Powell Eyring fluid over a rotating disk, *Taiwan Institute of chemical Engineers,* **45**, 2859-2867, 2014.
21. N. A. Khan, F. Riaz and S. Khan, Analytic approximate solutions and numerical results for stagnation point flow of Jeffrey fluid towards an off-centered rotating disk, *Journal of Mechanics,* **31**, 201-215, 2015.
22. S. J. Liao, The proposed homotopy analysis techniques for the solution of nonlinear problems, Ph.D. Dissertation, *Shanghai Jiao Tong University*, Shanghai, 1992.
23. S. J. Liao, A uniformly valid analytic solution of two-dimensional viscous flow over a semi-infinite flat plate, *Journal of Fluid Mechanics,* **385**, 101-128, 1999.
24. N. A. Khan, F. Sultan, On the double diffusive convection flow of Eyring-Powell fluid due to cone through a porous medium with Soret and Dufour effects, *AIP Advances*, **5**, 057140, 2015.
25. N. A. Khan, F. Riaz, F. Sultan, Effects of chemical reaction and magnetic field on a couple stress fluid over a non-linearly stretching sheet, *The European Physics Journal-Plus,* **129**, Art. ID 18, 2014.
26. F. M. White, Viscous fluid flow, 2nd edition, *McGraw-Hill,* New York.